

Distinguishing Electronic and Vibronic Coherence in 2D Spectra by Their Temperature Dependence

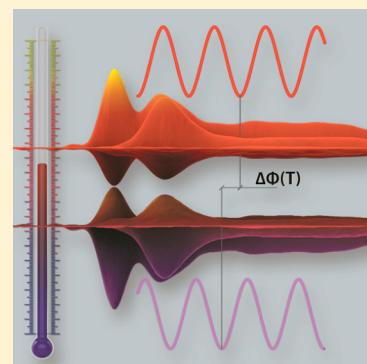
Václav Perlík,[†] Craig Lincoln,[‡] František Šanda,^{*,†} and Jürgen Hauer[‡]

[†]Institute of Physics, Faculty of Mathematics and Physics, Charles University, Ke Karlovu 5, Prague 121 16, Czech Republic

[‡]Photonics Institute, Vienna University of Technology, Gusshausstrasse 27, 1040 Vienna, Austria

Supporting Information

ABSTRACT: Long-lived oscillations in 2D spectra of chlorophylls are at the heart of an ongoing debate. Their physical origin is either a multipigment effect, such as excitonic coherence, or localized vibrations. We show how relative phase differences of diagonal- and cross-peak oscillations can distinguish between electronic and vibrational (vibronic) effects. While direct discrimination between the two scenarios is obscured when peaks overlap, their sensitivity to temperature provides a stronger argument. We show that vibrational (vibronic) oscillations change relative phase with temperature, while electronic oscillations are only weakly dependent. This highlights that studies of relative phase difference as a function of temperature provide a clear and easily accessible method to distinguish between vibrational and electronic coherences.



SECTION: Spectroscopy, Photochemistry, and Excited States

In the early stage of photosynthesis, excitation is created by absorption of a photon, followed by exciton migration from the peripheral antenna complexes to the reaction center with remarkably high efficiency.¹ Extension of 2D spectroscopy² to the visible domain provided fresh impetus to photosynthesis research when Engel et al.³ reported oscillations in the 2D spectra of the Fenna–Mathews–Olson (FMO) complex of bacteriochlorophylls. These oscillations survive over a picosecond and were ascribed to beating between delocalized excitonic (electronic) states.³ The picosecond lifetime is unexpected for electronic coherence, and despite attempts at explanation by adopting less common relaxation theories,⁴ such longevity sparked a still ongoing debate about the nature of the underlying coherence phenomena. Engel et al.³ speculated that the surrounding protein shields the electronic coherence from dephasing interaction with the solvent environment. Low-frequency vibrations on individual pigments, the alternative readily explaining the observed lifetimes, were ruled out because of the observed out-of-phase (180°) difference between the diagonal and antidiagonal peak widths as a function of population time.

Nonetheless, the original argument triggered a critical discussion^{5–14} as it quickly became understood that the out-of-phase oscillatory pattern of diagonal and cross peaks cannot serve as a strong criterion for the identification of electronic coherence. For example, Christensson et al.⁵ showed that it depends strongly on excitation conditions, that is, the overlap between absorption and excitation spectra. Cheng and Fleming⁶ showed that electronic and vibrational coherences can be distinguished by comparison of the rephasing (R) and

nonrephasing (NR) portions of a 2D signal, where electronic beatings will only appear as oscillations on the NR diagonal peaks and on R cross peaks. Contrastingly, vibrational coherences do not show similar specificity, and oscillations can be present for both NR and R signals for any peak position (Figure 1). Experiments supported this view.⁷ Other studies ruled out the purely electronic Frenkel excitons to be consistent with all observed features of FMO.⁸ There are two concerns about Cheng's approach:^{9,10} (i) Purely R and NR spectra can only be obtained with δ -pulses, that is, with finite pulses, the two signals are, to some extent, always mixed and (ii) the current state of discussion accepts the important role of vibrations, even in primarily electronic scenarios, as they can support long-lived electronic coherences in FMO by means of vibronic dynamics.^{11,12} Formally, the argument by Cheng and Fleming is based on comparing a four-level system (4LS) of vibrational character with a three-level system (3LS) of electronic character. In vibronic systems, electronic coupling can redistribute dipole strength to enhance excited-state over ground-state coherences¹³ or vice versa.¹⁴ This results in a 3LS response pattern, which can explain all experimental findings in FMO,¹³ without the need to invoke long-lived electronic coherences.

To follow recent discussions, electronic (E), vibrational (V), and vibronic (P) model dynamics shall be specified. Constituting chromophores ($i = 1, 2$) of the electronic dimer

Received: November 15, 2013

Accepted: January 7, 2014

Published: January 7, 2014

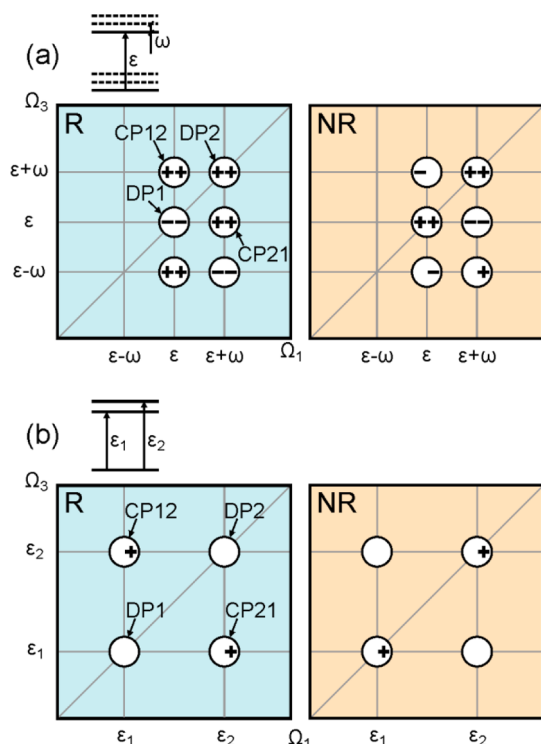


Figure 1. (a) Schematic 2D map of oscillatory phases for a vibrational system (eq 2), showing the part of the spectra related to the first two vibrational levels above the ground and excited states. Signals oscillate as $A \mp B \cos \omega t_2$, $B > 0$. The relevant sign is indicated at the left side of the circles for ground-state bleach (GSB) and the right for stimulated emission (SE). The absence of a sign indicates vanishing oscillations $B = 0$. R and NR denote rephasing and nonrephasing spectra, respectively. (b) The peak structure and oscillatory phases of the form $A \mp B \cos[(\varepsilon_2 - \varepsilon_1)t_2]$, $B > 0$ for an electronic dimer (eq 1).

(E) are treated as two-level electronic systems with transition frequency ε^i between the ground $|g^i\rangle$ and excited $|e^i\rangle$ electronic states with $\hat{H}_e^i = \hbar \varepsilon^i |e^i\rangle\langle e^i|$. We adopt many-body notation by introducing creation operators of exciton $\hat{A}^i = |e^i\rangle\langle g^i|$ and their annihilation adjoints \hat{A}^i . The two chromophores are coupled by resonant (dipole–dipole) interaction $\hbar J$. In the Heitler–London approximation, the excitation of one chromophore is accompanied by de-excitation of the other, resulting in the dimer Hamiltonian

$$\hat{H}_E = \sum_{i=1}^2 \hat{H}_e^i + \hbar J (\hat{A}^{1\dagger} \hat{A}^2 + \hat{A}^{2\dagger} \hat{A}^1) + \hbar Y \hat{A}^{1\dagger} \hat{A}^2 \hat{A}^1 \hat{A}^2 \quad (1)$$

where Y is a double-excitation frequency shift.

Underdamped vibrations were modeled by a harmonic oscillator of frequency ω^i with displacement d^i between ground- and excited-state potential surfaces of the chromophore

$$\hat{H}_V^i = \left[\frac{\hat{p}^{i2}}{2m} + \frac{1}{2} m \omega^{i2} \hat{q}^{i2} \right] |g^i\rangle\langle g^i| + \left[\frac{\hat{p}^{i2}}{2m} + \frac{1}{2} m \omega^{i2} (\hat{q}^i - d^i)^2 \right] |e^i\rangle\langle e^i| \quad (2)$$

The simplest model of vibrational dynamics (V) assumes a single chromophore modulated by a vibration $\hat{H}_V = \hat{H}_e^1 + \hat{H}_V^1$.

Interplay between resonant coupling in the dimer (eq 1) and underdamped on-site vibrations (eq 2) induces vibronic dynamics (P)

$$\hat{H}_P = \hat{H}_E + \sum_{i=1}^2 \hat{H}_V^i \quad (3)$$

Vibrations of eq 2 are damped in Landau–Teller relaxation,¹⁵ that is, coupled to a local bath¹⁶ of spectral density $\zeta(\omega) = \lambda \Lambda \omega / (\omega^2 + \Lambda^2)$, where Λ is the relaxation rate and λ the reorganization energy. The electronic dimer (E) is similarly supplemented with local spectral diffusion (see Supporting Information S2). However, the specific choice of a bath model and its parametrization are not crucial for our conclusion.¹⁷

The dynamics of 2D spectra is a combination of population transfer and line shape effects (pure dephasing), induced by bath fluctuations of the Hamiltonian's eigenstates and eigenvalues, respectively.¹⁸ Here, they are treated in the spirit of Zhang et al.¹⁹ The population transport between eigenstates is thus described by a quantum master equation. Line shape effects are accounted for using the second cumulant.¹⁸ Calculations are performed at finite temperature T , taking into account detailed balance, required for the master equation, and the fluctuation–dissipation theorem for cumulants.

We start the discussion of oscillatory components of 2D spectra with a qualitative diagrammatic analysis²⁰ for ground-state bleach (GSB) and stimulated emission (SE) pathways. For simplicity, interference from the excited-state absorption (ESA) pathways is formally neglected by introduction of a large biexciton frequency shift $Y \rightarrow \infty$. The inclusion of ESA pathways typically results in weaker total signals but leaves the oscillatory phases unchanged.²¹

The 2D peak structures for a vibrational and an electronic system are compared in Figure 1. We show the two lowest vibrational peaks (and related cross peaks), that is, Figure 1a refers to the vibrational 4LSs of refs 6 and 20, whereas the electronic dimer in Figure 1b comprises a unique ground state and two electronic excitons (eq 1). 2D peaks red-detuned from the lowest frequency of absorption (ε) require the existence of an energy level above the electronic ground state (Figure 1a) and serve as evidence of a ground-state vibrational level.

Figure 1 also illustrates the capacity of the detection frequency integrated pump–probe (PP) to discriminate between E and V dynamics suggested by Yuen-Zhou et al.²² Peaks with opposite phase will interfere destructively when the signal is integrated over Ω_1 (i.e., a PP signal) and over Ω_3 (i.e., a detection frequency integrated PP signal). As a result, all oscillations cancel in the V model of Figure 1a. In contrast, the electronic coherence of Figure 1b reveals in-phase oscillations that are retained after Ω_1 and Ω_3 integration. In short, comparison of Ω_3 -integrated PP and 2D signals can serve as a means to separate electronic and vibrational coherences, in agreement with the wavepacket formalism of Yuen-Zhou et al.²²

The diagrammatic framework²⁰ underlying the phases in Figure 1 results always in predictions of in/out-of-phase oscillations. More general phase shifts of the form $A + B \cos(\omega t_2 + \phi)$ can only be explained by bypassing the assumptions behind the methodology used by ref 20. Arbitrary phase shifts were obtained after avoiding the secular form of transport equations²³ and invoking nonstandard population to coherence transport. Within such a framework, the $\Delta\phi \equiv \phi_{DP2} - \phi_{CP21} = 90^\circ$ phase shift, observed in FMO, was interpreted as evidence for “quantum transport”,²⁴ that is, it was argued that it

indicates dynamical connection between population and coherence elements of the density matrix. We hereafter examine alternative explanations for a 90° phase difference. The analysis of ref 24 disregards effects from peak overlap, but as we will show, phase differences heavily depend on such overlaps.

In Figure 2a and b, we demonstrate the emergence of phase shifts when vibrational peaks are overlapping (details of the

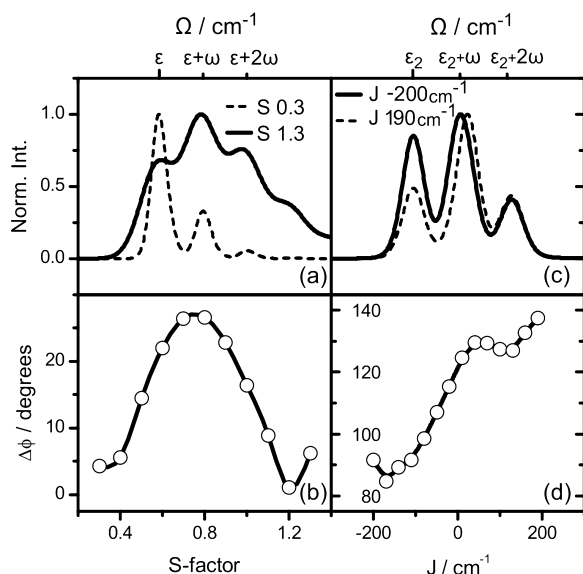


Figure 2. Left panels: Vibrational modulation of a single chromophore; (a) absorption spectra and (b) relative phase ($\Delta\phi \equiv \phi_{\text{DP2}} - \phi_{\text{CP21}}$) between DP2 and CP21 peaks of 2D rephasing spectra as a function of Huang–Rhys factor S . Parameters: $\varepsilon = 16000 \text{ cm}^{-1}$ and $\omega = 1400 \text{ cm}^{-1}$. Right panels: Vibronic dimer near resonance $\varepsilon_1 \cong \varepsilon_2 + \omega$; (c) absorption spectrum and (d) relative phase ($\Delta\phi$) between DP2 and CP21 peaks of rephasing spectra as a function of resonant coupling J in a vibronic dimer (eq 3). Dipoles of both chromophores are parallel and of the same value. Bath parameters, $T = 300 \text{ K}$, $\lambda = 600 \text{ cm}^{-1}$, and $\Lambda = 100 \text{ cm}^{-1}$, are the same for all panels.

phase retrieval procedure can be found in the Supporting Information S1). Overlap was controlled by the Huang–Rhys factor $S = d^2 m \omega / 2 \hbar$, which scales linearly with peak width for Landau–Teller relaxation dynamics. For small overlap ($S \rightarrow 0$), the 2D maps depicted in Figure 1 are reproduced, that is, $\Delta\phi \rightarrow 0$. Increasing S broadens peaks (Figure 2a), and spectral overlap between adjacent absorption peaks results in complex interferences, which significantly affect $\Delta\phi$ (Figure 2b). Peaks DP2 and CP21 no longer oscillate in phase, and $\Delta\phi$ varies significantly between 0 and approximately 30° . With a further increase of S , the dipole strength is redistributed to higher vibrational levels (see Figure 2a), and as a result, $\Delta\phi$ decreases again for $S \gtrsim 0.8$. We note that the V model does not reproduce large phase shift, such as the 90° reported in FMO.²⁴ A purely vibrational origin of the oscillations in FMO can therefore be rejected.

However, larger phase variations are observed upon introduction of vibronic dynamics (Figures 2c,d). The vibronic dimer (eq 3) was parametrized as a donor–acceptor system, where the acceptor’s transition frequency is red-shifted from the donor by about one vibrational quantum $\varepsilon_1 \cong \varepsilon_2 + \omega$. Thus, the vibrational ground state at $|e_1\rangle$ and the first excited level at $|e_2\rangle$ are resonant and covered by one peak in the absorption spectrum. Increasing coupling J redistributes the strength of

transition dipoles and affects the retrieved values of $\Delta\phi$. Variation of J allows one to obtain arbitrary values of $\Delta\phi$, including $\Delta\phi = 90^\circ$, without the need to invoke the quantum transport dynamics of ref 23. $\Delta\phi$ deviating from 0 or 180° is thus not indicative for electronic coherence as peak overlaps in vibronic systems yield similar effects.

The strong variations of phases observed in Figure 2 result from overlapping peaks DP1 and CP21 carrying opposite phases (Figure 1a). In contrast, all peaks of the electronic case oscillate in-phase (Figure 1b). This suggests, for an electronic system, independence of $\Delta\phi$ on absorption peak overlap, namely, for the total (R + NR) 2D signal. Similar ideas underlie recent observations that vibrational and electronic coherence show distinctly different behavior upon increasing disorder.²⁵ Here, we refine this idea into a readily accessible experimental variable to distinguish the two scenarios, namely, temperature T .

In Figure 3, we compare the temperature dependence of absorption spectra and $\Delta\phi$ for an electronic (Figure 3a,b) and a

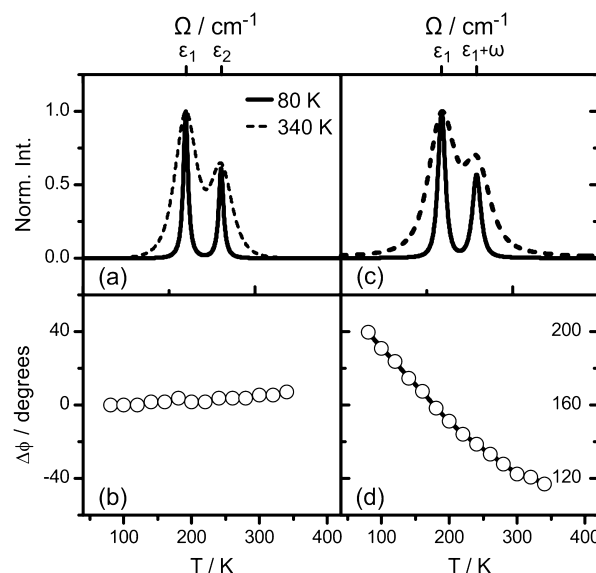


Figure 3. Temperature-dependent absorption spectra and $\Delta\phi$ for (a,b) electronic and (c,d) vibronic systems. Simulations are based on the total (R + NR) 2D signal. Parameters: Electronic dimer (eq 1): $\varepsilon_1 = 16000 \text{ cm}^{-1}$, $\varepsilon_2 = 16200 \text{ cm}^{-1}$, $J = -50 \text{ cm}^{-1}$, $\lambda = 25 \text{ cm}^{-1}$, $\Lambda = 80 \text{ cm}^{-1}$. Vibronic dimer (eq 3): $\varepsilon_1 = \varepsilon_2 = 16000 \text{ cm}^{-1}$, $\omega = 200 \text{ cm}^{-1}$, $J = -30 \text{ cm}^{-1}$, $\lambda = 20 \text{ cm}^{-1}$, $\Lambda = 40 \text{ cm}^{-1}$, $S = 0.8$.

vibronic (Figure 3c,d) dimer. Chromophores of the P model (eq 3) were chosen to be symmetric, $\varepsilon_1 = \varepsilon_2$, with vibrational frequency ω corresponding to the energy splitting of the E dimer. Vibrational structure was restricted to the two lowest levels and parametrized to yield similar absorption spectra for the E and P models at low temperatures.

A rise in temperature broadens absorption peaks and increases overlap similarly in panels a and c of Figure 3. The phase shift $\Delta\phi$, on the other hand, differs significantly. $\Delta\phi$ is only weakly dependent on T for an electronic dimer (Figure 3b), even when avoiding secular approximation, but T significantly changes $\Delta\phi$ for the vibronic system (Figure 3d). We analyzed the total (R + NR) 2D signal to avoid experimental ambiguities related to pulse overlap effects present in pure R (NR) spectra. Note, that their separate analysis would yield similar conclusions. Purely vibrational (V) coherence

exhibits similar temperature sensitivity as the vibronic case (P). We can thus discriminate them against the temperature-insensitive purely electronic dimer (E).

In conclusion, we have shown that vibrational, vibronic, and electronic oscillations in 2D maps show different phase sensitivity when absorption peaks overlap. In the case of coherences of vibrational or vibronic origin, $\Delta\phi$ may vary significantly, where purely electronic coherences are insensitive to temperature-induced peak broadening (see Figure 3a and b). The theoretical predictions made in this work can be readily verified by 2D measurements at different temperatures. Long-lived oscillatory beatings over a wide temperature range have already been reported for FMO.²⁶ Careful determination of $\Delta\phi$ between cross and diagonal peaks in such measurements will help to distinguish between electronic and vibronic coherences. Thus, 2D electronic spectroscopy is capable of determining the origin of oscillatory signals by the temperature dependence of relative phase differences $\Delta\phi$.

■ ASSOCIATED CONTENT

● Supporting Information

Notes on phase retrieving procedure and details about implemented relaxation and transport dynamics. This material is available free of charge via the Internet at <http://pubs.acs.org>.

■ AUTHOR INFORMATION

Corresponding Author

*E-mail: sanda@karlov.mff.cuni.cz.

Notes

The authors declare no competing financial interest.

■ ACKNOWLEDGMENTS

C.L. and J.H. acknowledge funding by the Austrian Science Fund (FWF): START project Y 631-N27. F.S. and V.P. acknowledge funding by the Czech Science Foundation (Grant No. 205/10/0989).

■ REFERENCES

- (1) Van Amerongen, H.; Valkunas, L.; Van Grondelle, R. *Photosynthetic Excitons*; World Scientific: Singapore, 2000.
- (2) Jonas, D. M. Two-Dimensional Femtosecond Spectroscopy. *Annu. Rev. Phys. Chem.* **2003**, *54*, 425–463.
- (3) Engel, G. S.; Calhoun, T. R.; Read, E. L.; Ahn, T.-K.; Mancal, T.; Cheng, Y.-C.; Blankenship, R. E.; Fleming, G. R. Evidence for Wavelike Energy Transfer through Quantum Coherence in Photosynthetic Systems. *Nature* **2007**, *446*, 782–786.
- (4) Pachón, L. A.; Brumer, P. Physical Basis for Long-Lived Electronic Coherence in Photosynthetic Light-Harvesting Systems. *J. Phys. Chem. Lett.* **2011**, *2*, 2728–2732.
- (5) Christensson, N.; Milota, F.; Hauer, J.; Sperling, J.; Bixner, O.; Nemeth, A.; Kauffmann, H. F. High Frequency Vibrational Modulations in Two-Dimensional Electronic Spectra and Their Resemblance to Electronic Coherence Signatures. *J. Phys. Chem. B* **2011**, *115*, 5383–5391.
- (6) Cheng, Y. C.; Fleming, G. R. Coherence Quantum Beats in Two-Dimensional Electronic Spectroscopy. *J. Phys. Chem. A* **2008**, *112*, 4254–4260.
- (7) Turner, D. B.; Wilk, K. E.; Curmi, P. M. G.; Scholes, G. D. Comparison of Electronic and Vibrational Coherence Measured by Two-Dimensional Electronic Spectroscopy. *J. Phys. Chem. Lett.* **2011**, *2*, 1904–1911.
- (8) Sharp, L. Z.; Egorova, D.; Domcke, W. Efficient and Accurate Simulations of Two-Dimensional Electronic Photon-Echo Signals: Illustration for a Simple Model of the Fenna–Matthews–Olson Complex. *J. Chem. Phys.* **2010**, *132*, 014501.
- (9) Mancal, T.; Christensson, N.; Lukes, V.; Milota, F.; Bixner, O.; Kauffmann, H. F.; Hauer, J. System-Dependent Signatures of Electronic and Vibrational Coherences in Electronic Two-Dimensional Spectra. *J. Phys. Chem. Lett.* **2012**, *3*, 1497–1502.
- (10) Milota, F.; Prokhorenko, V. I.; Mancal, T.; von Berlepsch, H.; Bixner, O.; Kauffmann, H. F.; Hauer, J. Vibronic and Vibrational Coherences in Two-Dimensional Electronic Spectra of Supramolecular J-Aggregates. *J. Phys. Chem. A* **2013**, *117*, 6007–6014.
- (11) Chin, A. W.; Prior, J.; Rosenbach, R.; Caycedo-Soler, F.; Huelga, S. F.; Plenio, M. B. The Role of Non-Equilibrium Vibrational Structures in Electronic Coherence and Recoherence in Pigment–Protein Complexes. *Nat. Phys.* **2013**, *9*, 113–118.
- (12) Sharp, L. Z.; Egorova, D. Towards Microscopic Assignment of Oscillative Signatures in Two-Dimensional Electronic Photon-Echo Signals of Vibronic Oligomers: A Vibronic Dimer Model. *J. Chem. Phys.* **2013**, *139*, 144304.
- (13) Christensson, N.; Kauffmann, H. F.; Pullerits, T.; Mancal, T. Origin of Long-Lived Coherences in Light-Harvesting Complexes. *J. Phys. Chem. B* **2012**, *116*, 7449–7454.
- (14) Tiwari, V.; Peters, W. K.; Jonas, D. M. Electronic resonance with Anticorrelated Pigment Vibrations Drives Photosynthetic Energy Transfer Outside the Adiabatic Framework. *Proc. Natl. Acad. Sci. U.S.A.* **2013**, *110*, 1203–1208.
- (15) Landau, L. D.; Teller, E. Zur Theorie der Schalldispersion (Theory of Sound Dispersion). *Phys. Z. Sowjetunion* **1936**, *10*, 34–43.
- (16) Šanda, F. The Instability in the Long-Time Regime Behaviour of a Kinetic Model. *J. Phys. A* **2002**, *35*, 5815–5831.
- (17) Butkus, V.; Valkunas, L.; Abramavicius, D. Molecular Vibrations-Induced Quantum Beats in Two-Dimensional Electronic Spectroscopy. *J. Chem. Phys.* **2012**, *137*, 044513.
- (18) Mukamel, S.; Abramavicius, D.; Palmieri, B.; Voronine, D. V.; Šanda, F. Coherent Multidimensional Optical Spectroscopy of Excitons in Molecular Aggregates; Quasiparticle versus Supermolecule Perspectives. *Chem. Rev.* **2009**, *109*, 2350–2408.
- (19) Zhang, W. M.; Meier, T.; Chernyak, V.; Mukamel, S. Exciton-Migration and Three-Pulse Femtosecond Optical Spectroscopies of Photosynthetic Antenna Complexes. *J. Chem. Phys.* **1998**, *108*, 7763–7774.
- (20) Butkus, V.; Zigmantas, D.; Valkunas, L.; Abramavicius, D. Vibrational vs. Electronic Coherences in 2D Spectrum of Molecular Systems. *Chem. Phys. Lett.* **2012**, *545*, 40–43.
- (21) Kreisbeck, C.; Kramer, T.; Aspuru-Guzik, A. Disentangling Electronic and Vibronic Coherences in Two-Dimensional Echo Spectra. *J. Phys. Chem. B* **2013**, *117*, 9380–9385.
- (22) Yuen-Zhou, J.; Krich, J. J.; Aspuru-Guzik, A. A Witness for Coherent Electronic vs Vibronic-Only Oscillations in Ultrafast Spectroscopy. *J. Chem. Phys.* **2012**, *136*, 234501.
- (23) Redfield, A. G. On the Theory of Relaxation Processes. *IBM J. Res. Dev.* **1957**, *1*, 19–31.
- (24) Panitchayangkoon, G.; Voronine, D. V.; Abramavicius, D.; Caram, J. R.; Lewis, N. H. C.; Mukamel, S.; Engel, G. S. Direct Evidence of Quantum Transport in Photosynthetic Light-Harvesting Complexes. *Proc. Natl. Acad. Sci. U.S.A.* **2011**, *108*, 20908–20912.
- (25) Butkus, V.; Zigmantas, D.; Abramavicius, D.; Valkunas, L. Distinctive Character of Electronic and Vibrational Coherences in Disordered Molecular Aggregates. *Chem. Phys. Lett.* **2013**, *587*, 93–98.
- (26) Panitchayangkoon, G.; Hayes, D.; Fransted, K. A.; Caram, J. R.; Harel, E.; Wen, J. Z.; Blankenship, R. E.; Engel, G. S. Long-Lived Quantum Coherence in Photosynthetic Complexes at Physiological Temperature. *Proc. Natl. Acad. Sci. U.S.A.* **2010**, *107*, 12766–12770.